

MULTI-FREQUENCY, MULTI-POLARIZATION EXTERNAL CALIBRATION OF SIR-C/XSAR

Final Report NASA/JPL GRANT JPL-958749

Submitted to :
Jet Propulsion Laboratory
ATTN: Dr. Anthony Freeman
4800 Oak Grove Drive
Pasadena, CA 91109

Prepared by:
Prof. Kamal Sarabandi (PI)

Radiation Laboratory
Department of Electrical Engineering and Computer Science
The University of Michigan
Ann Arbor, MI 48109-2122
Tel: (313) 764-0500
Fax: (313) 747-2106

Project Management:
K. Sarabandi, M.C. Dobson, L. Pierce, F.T. Ulaby

RL-988 = RL-988

Contents

1	Introduction	3
2	Calibration Experiment	4
3	SUMMARY OF ACCOMPLISHMENTS	10
3.1	Calibration Algorithms For Point Targets	10
3.2	Measurement and Calibration of Differential Mueller Matrices	11
3.3	Characterization and Design of Precision Active Calibration Targets	11
3.4	Analysis, Design, and Construction of an Optimum Corner Reflector	12
3.5	Calibration Algorithms for Polarimetric SAR Systems	13
3.6	Cross Calibration Experiment	13
3.7	Applications	13
4	Students Supported	14
5	Publications	14
6	Appendices A-H	15

MULTI-FREQUENCY, MULTI-POLARIZATION EXTERNAL CALIBRATION OF SIR-C/XSAR

Abstract

In this final report a summary of our activities with regard to external calibration of the Shuttle Imaging Radar-C/XSAR (SIR-C/XSAR) is provided. The University of Michigan was involved in the development of calibration procedures and precision calibration devices to quantify the complex radar images with an accuracy of 0.5 dB in magnitude and 5 degrees in phase. Our research activities in the area of calibration of polarimetric SARs can be categorized into five areas: (1) development of calibration techniques for point targets, (2) development of polarimetric calibration techniques for distributed targets, (3) design of novel precision calibration targets, (4) development of polarimetric calibration techniques for SAR systems based on point and distributed targets, and (5) application of calibrated images for remote sensing of vegetation and soil moisture.

On April 9, and September 30, 1994 the SIR-C/XSAR instruments were launched twice, each time on an 11-day mission, aboard the NASA space shuttle Endeavor. During both missions several supersites received frequent overflights including the Raco supersite in the upper peninsula of Michigan. The Raco supersite, centered on 46.392 N. Latitude and 84.885 W. Longitude, is located in Chippewa County in the eastern part of Michigan's Upper Peninsula. The area under study and imaged in the SIR-C/X-SAR crossover region is approximately 20 km E-W and 20 km N-S. This site was imaged twelve times between April 9 and April 19 and twelve time between September 30 and October 10. A team consisting of scientists and graduate students were involved in deployment of targets and collection of ancillary data.

1 Introduction

In radar remote sensing, calibration of polarimetric radar systems is of great importance because the success of any inversion algorithm or any radar classifier depends directly on the accuracy of the measured data. To provide a quantitative value for the measured backscatter and remove the distortion from different channels of the radar caused by the active components and the antenna, an external calibration must be performed. The external calibration of a radar system involves a comparison of the measured response of the unknown target with the measured response of one or more calibration targets of the known radar cross section. For this purpose appropriate calibration targets and convenient calibration algorithms are required. A metallic sphere is a desirable calibration target because it is one of the few geometries for which an analytical RCS exist and its backscatter cross section is independent of orientation angle. However, the drawback of a metallic sphere is its

relatively small RCS. In calibration of images acquired from SAR using point calibration targets, the RCS of the calibration targets must be much larger than those of the surrounding pixels in the image. This requirement ensures that the radar return from the background is negligible relative to the return from the calibration target. In practice the RCS of calibration targets for imaging radars can be measured using the metallic sphere.

The following characteristics are desirable for calibration targets of imaging radars: (1) large RCS, (2) wide RCS pattern (being insensitive to orientation angle), (3) easily deployable (having small physical size), (4) stable RCS, and (5) insensitive RCS to its background (no interaction with its surrounding). Accurate measurement of scattering matrices of calibration targets for SARs requires accurate calibration techniques for point targets. Once the calibration targets are designed and fully characterized, a calibration algorithm for the SAR image based on the point calibration targets is required. The accuracy of the overall calibration procedure must then be checked by comparing the calibrated image to the measurement of an independent calibrated instrument such as a truck-mounted scatterometer system. Therefore a calibration procedure for distributed targets for nonimaging radars is also needed.

In any backscatter measurement of distributed targets the quantities of interest are the backscatter coefficients, which are the second moments of the scattered field per unit area. Calibration algorithms based on point targets for synthetic aperture radars must infer the calibration constant for backscattering coefficients from the RCS of the point targets. This process requires accurate knowledge of the SAR impulse function which is very difficult to characterize. To circumvent this problem calibration algorithms based on known distributed targets can be used. Such a calibration algorithm, however, provides the calibrated differential Mueller matrix of a region of the image as opposed to calibrated pixels. In what follows we briefly describe the calibration experiments and then we summarize the techniques and devices developed during the course of this investigation.

2 Calibration Experiment

In this section a brief description of our field activities during both SIR-C missions is given. Figure 1 shows the location of the Raco supersite where all of our calibration activities took place. The overall goal throughout the duration of the SIR-C/X-SAR project has been the development of image calibration algorithms by determining extracting the effects of system distortion parameters from the SIR-C polarimetric radar images. The objectives and methods used for assuring accurate calibration for both SIR-C missions were as follows:

1. Design and development of appropriate point calibration targets.

2. Characterization of RCS of point targets.
3. Deploy and monitor the point targets in the calibration site.
4. Development and assessment of polarimetric calibration algorithms using point point calibration targets.
5. Development of a procedure that would allow calibration of the imaging radars using distributed targets.
6. Deployment and measurement of backscatter for area extended targets with calibrated polarimetric scatterometer system.
7. Absolute calibration of SIR-C/X-SAR imagery acquired at L,C, and X bands
8. Accurate calibration over the geographical extent of the imaged scenes

During the SIR-C flights point calibration targets were distributed in open areas within the area imaged by the sensors. Both passive and active targets were deployed. For the April mission six 1.07 m trihedrals and one C-band PARC were located at the Rifle Range near the Raco Airfield. Two 2.4 m trihedrals were located at the Raco Airfield. Four 2.4 m trihedrals, one L-band single antenna polarimetric active radar calibrator (SAPARC'), one C-band SAPARC, and one C-band PARC were located at Cryderman Field. See Figure 2 for the location of these fields.

Details regarding target positioning, including gps derived coordinates, target type, and measured elevation angles and azimuths, can be found in Table 1. The three target locations are depicted on the map SIR-C/X-SAR Test Stands and Calibration Sites. Targets were repositioned and/or monitored for accurate positioning before each overflight using electronic levels and Brunton compasses. Scatterometer measurements were made at L, C, and X-bands in conjunction with each SIR-C/X-SAR overpass. These measurements were made at Cryderman field.

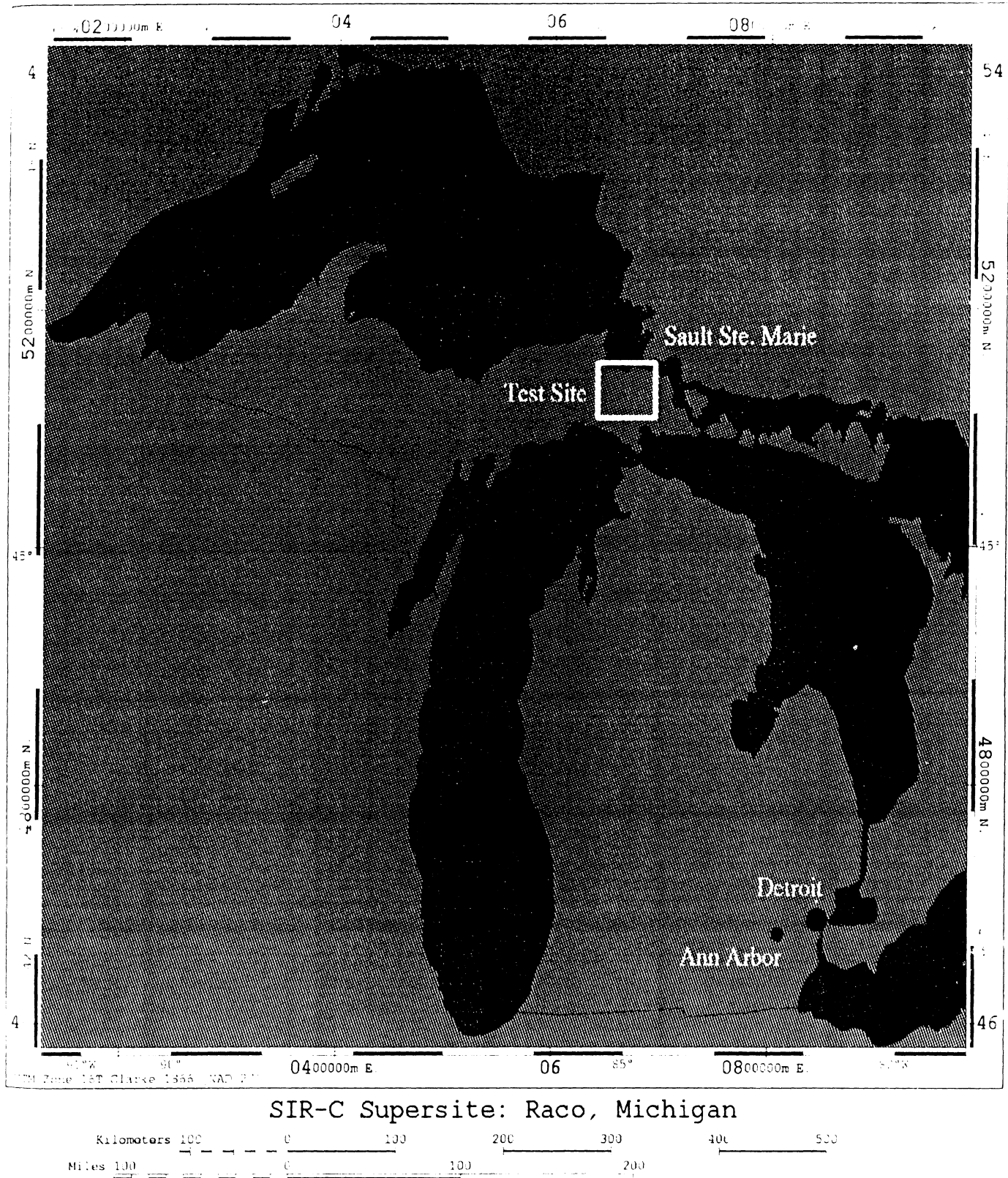
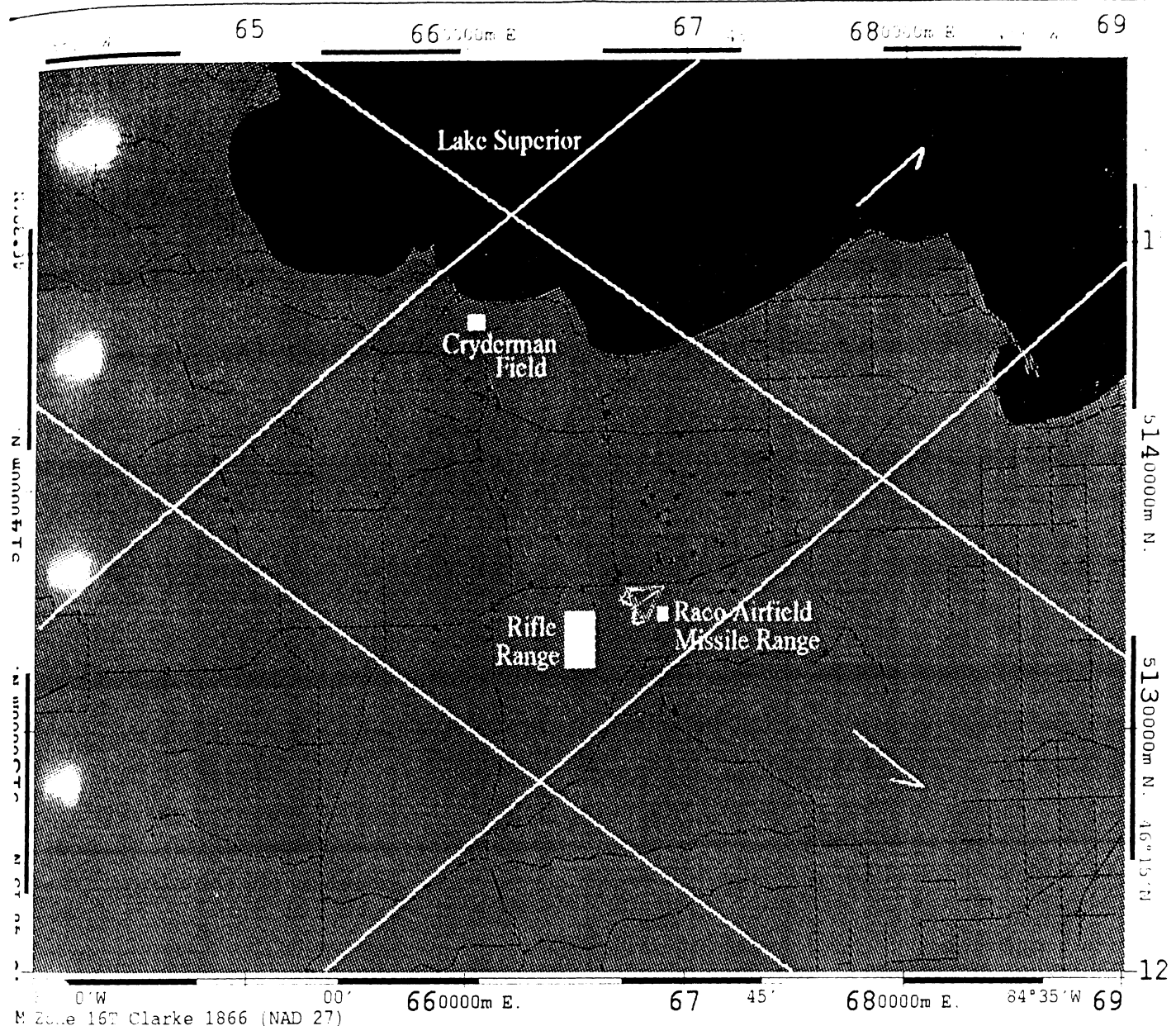
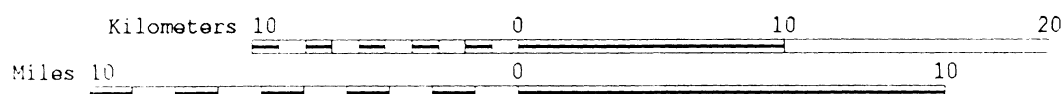


Figure 1: Raco SIR-C/XSAR supersite.



SIR-C Test Stands and Calibration Sites

Raco, Michigan Supersite



- | | |
|---|--------------------|
| | Forest test stands |
| | Calibration sites |
| | SIR-C imaged swath |

Figure 2: Location of test fields in Raco SIR-C/XSAR supersite.

Table 1: Calibration Targets

Calibration Target Plan at Raco Supersite April 1994 Mission							MET (dd/mm:ss)	00/07:50:29	01/07:32:17
							Orbit No.	22	22.2
							Data-Take No.	D	D
							Ascending/Descending	S	S
							North/South Looking (from Shuttle)	30.14	19.33
							Look Angle (relative to SIR-C)	31.387	20.132
							Local Incidence Angle	127.461	128.428
							SIR-C Azimuth Heading (True North)	127.86	127.86
							Target Azimuth (True North)	N	N
							Target Looking (N/S)	134	134
							Target Azimuth (Mag. North)	134	134
							Elevation Angles (From horizontal)	Elevation Angles (From horizontal)	Elevation Angles (From horizontal)
							Azimuth (from True north)	Azimuth (from True north)	Azimuth (from True north)
							Level (degrees)	Level (degrees)	Level (degrees)
RIFLE RANGE							Target Type	Size (cm)	Max. RCS (dBm^2)
T2-1	Target Name	/	Latitude	Longitude			Trihedral	107	30.5
	Target Name	g					Trihedral	107	29.2
							Trihedral	107	29.6
							Trihedral	107	27.2
							Trihedral	107	30.0
							Trihedral	107	31.2
							C-PARC #2	42.4	31.4
PACO									
T1-5	Target Name	A/D	46.3468	-84.8058	Trihedral	240		30.3	128.9
		A/D			Trihedral	240			0.6
AIRFIELD									
CRYDERMAN FIELD	Target Name	A/D	46.4591	-84.9070	Trihedral	240		31.0	126.9
		A/D	46.4562	-84.9093	Trihedral	240		31.5	128.9
		A/D	46.4561	-84.9130	Trihedral	240		31.3	125.9
		A/D	46.4571	-84.9152	Trihedral	240		31.0	126.9
		A/D	46.4578	-84.9104	L-SAPARC	32.1		32.1	0.8
		A/D	46.4597	-84.9102	C-SAPARC			?	1.0
		A/D	46.4583	-84.9126	C-PARC #1	44.5		?	1.0
							Date	Saturday	Sunday
							Day	9-Apr	10-Apr
							Time	14:55:29	14:32:17

		04/00:25:22			05/00:05:44			05/06:15:43			05/23:45:41		
		66 66.2 A S 21.65 22.65 51.853 232.86 N			82 82.2 A S 29.53 30.849 52.341 232.86 N			86 86.4 D N 23.77 24.531 131.101 311.86 S			98 98.12 A S 35.512 36.801 52.911 232.86 N		
Site	Target Name	Elevation Angles (From horizontal)	Azimuth (from True north)	Level (degrees)	Elevation Angles (From horizontal)	Azimuth (from True north)	Level (degrees)	Elevation Angles (From horizontal)	Azimuth (from True north)	Level (degrees)	Elevation Angles (From horizontal)	Azimuth (from True north)	Level (degrees)
RIFLE RANGE	T2-1	30.6	53.9	0.1	30.2	236.9	0.1	30.9	310.9	0.2	9.9	232.4	0.4
	T2-2	31.6	53.9	0.9	30.6	233.9	0.1	30.0	313.9	0.3	9.9	233.4	0.4
	T2-3	29.6	54.9	0.5	28.5	234.9	0.2	29.9	315.9	0.4	9.9	232.4	0.1
	T2-4	29.6	52.9	0.7	29.2	237.9	-0.3	30.5	311.9	0.2	9.3	233.9	0.0
	T2-5	30.9	53.9	0.5	30.4	235.9	0.8	30.2	309.9	-0.2	10.1	233.9	0.1
	T2-6	30.5	53.9	0.9	30.7	233.9	1.2	30.5	311.9	1.0	10.2	232.9	0.0
	P4	20.7	52.9	0.1	30.8	232.9	0.1	24.5	311.9	0.0	36.8	232.9	0.0
	RACO	T1-5			30.5	231.9	0.4	30.1	311.9	0.1	9.8	232.8	0.2
AIRFIELD	T1-6				30.0	233.9	0.7	30.3	312.9	0.1	11.0	233.1	0.2
	CRYDEFMAN FIELD	T1-1	30.4	53.9	0.5	30.0	233.9	0.5	30.0	312.9	0.0	-	-
		T1-2	30.6	53.9	0.3	30.2	232.9	0.0	29.6	311.9	0.6	-	-
		T1-3	30.9	51.9	1.0	31.0	233.9	0.1	29.6	311.9	0.2	10.3	236.9
		T1-4	31.1	52.9	-0.6	31.1	232.9	0.7	30.0	311.9	0.4	11.1	232.9
		P1	21.6	51.9	0.5	30.9	232.9	0.8	24.9	312.9	0.1	35.1	239.9
		P2	23.4	52.9	ok	30.7	235.9	ok	24.8	310.9	ok	36.5	236.9
		P3	22.8	52.9	0.5	29.2	235.9	1.1	24.5	311.9	0.4	37.2	241.9
		Wednesday 13-Apr 7:30:22			Thursday 14-Apr 7:10:44			Friday 15-Apr 6:50:41					

		06/05:55:33			06/23:25:12			07/05:34:57			08/05:13:57		
		102 102.41 D N 30.701 31.747 131.674 311.86 S 318			114 114.1 A S 40.09 41.799 53.567 232.86 N 239			118 118.6 D N 35.903 37.268 131.959 311.86 S 318			134 134.3 D N 39.787 41.306 132.328 311.86 S 318		
Site	Target Name	Elevation Angles (From horizontal)	Azimuth (from True north)	Level (degrees)	Elevation Angles (From horizontal)	Azimuth (from True north)	Level (degrees)	Elevation Angles (From horizontal)	Azimuth (from True north)	Level (degrees)	Elevation Angles (From horizontal)	Azimuth (from True north)	Level (degrees)
RIFLE RANGE	T2-1	29.6	312.9	0.5	11.0	232.9	0.0	-	-	-	-	-	-
	T2-2	29.9	313.4	0.5	10.6	231.9	0.0	-	-	-	-	-	-
	T2-3	29.8	311.4	0.4	10.8	232.9	0.2	-	-	-	-	-	-
	T2-4	-	-	-	10.9	233.9	0.2	9.7	311.9	0.4	10.4	309.9	309.9
	T2-5	30.0	311.9	0.3	10.3	232.9	0.2	9.9	311.9	0.1	9.7	312.9	312.9
	T2-6	-	-	-	10.6	231.9	0.4	9.7	310.9	0.4	9.6	310.9	310.9
	P4	31.7	311.9	0.0	41.8	232.9	0.0	37.3	311.9	0.0	41.0	313.9	313.9
FACO	T1-5	29.3	313.4	0.4	9.3	234.7	0.3	-	-	-	-	-	-
	T1-6	30.4	311.9	0.1	10.6	232.7	0.3	10.7	313.9	1.0	18.7	317.9	317.9
AIRFIELD	T1-1	-	-	-	12.2	223.9	2.9	11.0	311.9	0.4	10.5	311.9	311.9
	T1-2	-	-	-	15.1	230.9	1.6	9.4	314.9	2.3	10.8	318.9	318.9
	T1-3	29.5	312.9	0.0	9.9	232.9	1.0	-	-	-	-	-	-
	T1-4	30.0	313.9	0.4	<2.0	41.7	232.9	2.0	7	?	42.0	312.9	312.9
	P1	31.0	310.9	ok	40.9	227.9	ok	37.0	312.9	ok	42.1	312.9	312.9
	P2	31.4	310.9	0.4	41.2	232.9	0.3	37.6	311.9	0.5	41.4	313.9	313.9
	P3	32.4	313.9										
		Friday 15-Apr 13:00:33			Saturday 16-Apr 6:30:12			Sunday 17-Apr 12:59:57			Sunday 17-Apr 12:18:57		

		09/04:52:22		09/22:20:59	
Site	Target Name	Elevation Angles (From horizontal)	Azimuth (from True north)	Level (degrees)	Elevation Angles (From horizontal)
RIFLE RANGE	T2-1				10.6
	T2-2				10.4
	T2-3				10.6
	T2-4	10.1	311.9	-0.3	
	T2-5	9.6	312.4	-0.1	
	T2-6	9.6	311.9	-0.6	
	P4	43.8	311.9	0.5	
PACO AIRFIELD	T1-5	10.0	59.6-14	0.0	10.0
	T1-6	10.0	311.9	0.0	
CRYDERMAN FIELD	T1-1	10.4	310.9	0.4	
	T1-2	10.4	318.9	1.5	
	T1-3	11.4	51.9	0.4	
	T1-4	10.8	51.9	1.2	
	P1	44.9	312.9	0.3	
	P2	44.2	313.9	?	
	P3	43.8	312.9	0.6	

Monday
18-Apr
11:57:22

Tuesday
19-Apr
5:25:59

In the October mission 21 calibration targets were positioned. Six 1.07 m trihedrals, one L-band SAPARC, one C-band SAPARC, and four 2.4 m trihedrals were located at the Rifle Range near the Raco Airfield. Two C-band PARCS were located at the Raco Airfield. Four 2.4 m trihedrals were located at Cryderman Field. In addition, three distributed targets areas were established at the Rifle Range. Details regarding point target positioning, including GPS derived coordinates, target type, and measured elevation angles and azimuths, can be found in Table 2 (October SIR-C/X-SAR Calibration Point Targets). Point targets were repositioned and/or monitored for accurate positioning before each overflight using electronic levels and Brunton compasses. During the 11-day mission, polarimetric scatterometers were used to collect data at L, C, and X-bands in conjunction with each SIR-C/X-SAR overpass. This data is used to define the average Mueller matrix of distributed targets. Three distributed targets, or surfaces, were defined and located at the rifle range. These were approximately 100 m X 100 m. Each plot (S1 to S3) had a distinctive surface roughness with RMS roughness ranging from 2 to 6 cm. (Tables 8 and 9). The locations of the distributed targets are documented on the map SIR-C/X-SAR October 1994 Rifle Range Distributed and Point Target Locations.

The details of experimentations and results are reported in [1] and [2] which are also given in Appendix A.

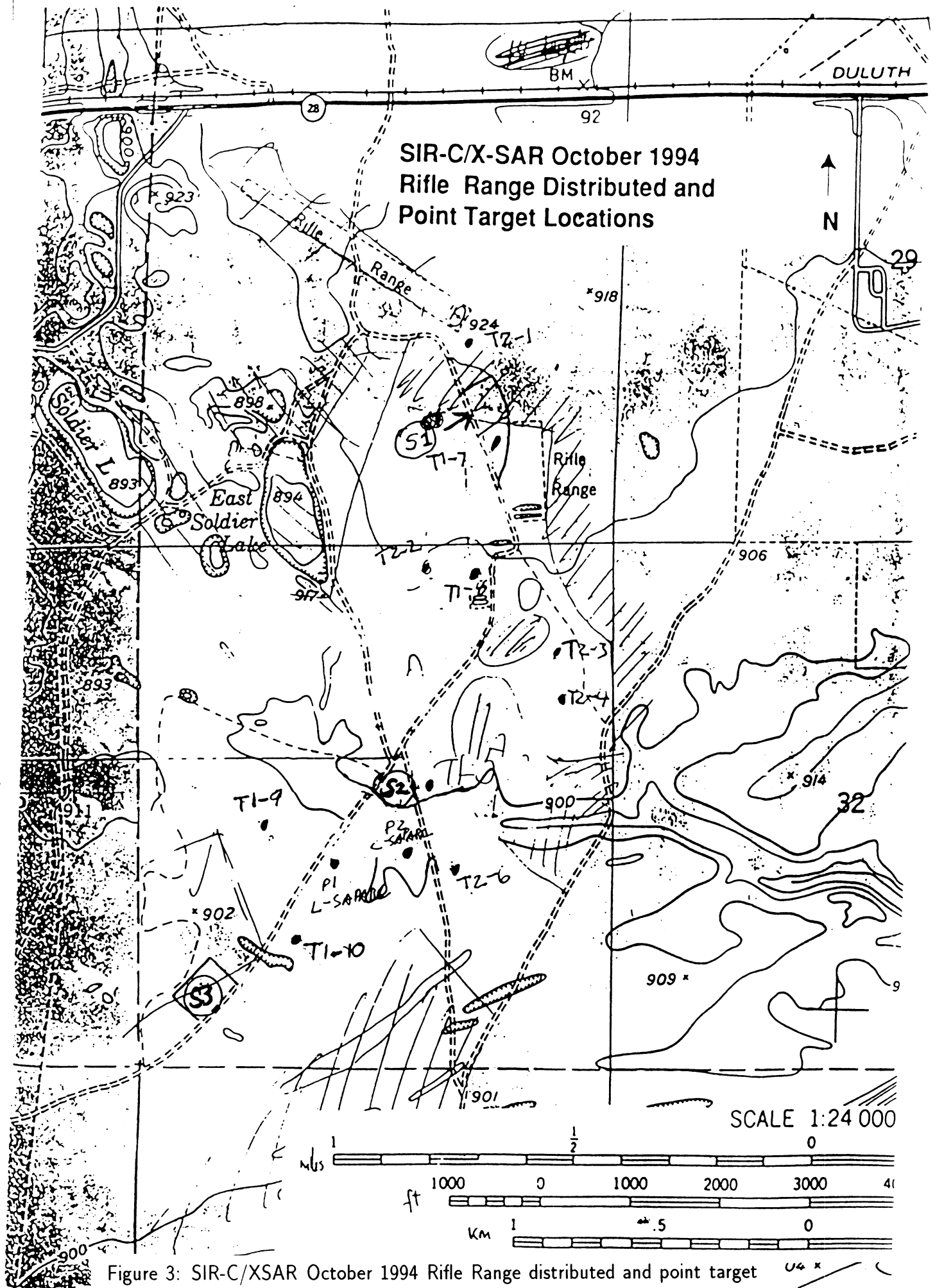


Figure 3: SIR-C/XSAR October 1994 Rifle Range distributed and point target locations.

Table 2

table6.formatted

Table 6: October SIR-C/X-SAR Calibration Point Targets

Rifle Range	P1	A/D	46.3481	-84.8487	L-SAPARC	Target Type	Size (cm)	Max RCS (dBm/2)	Elevation Angles (From horizontal)	Azimuth (from true north)	Level (degrees)	Elevation Angles (From horizontal)		Azimuth (from true north)	
												Level	Temp (°C) or Atten. (dB)	Level	
P2	A/D	A/D	46.3369	-84.8519	C-SAPARC	Trihedral	240	30.0	134.0	0.0	16°	0.0	21.2	0.0	134.0
T1-7	A/D	A/D	46.3360	-84.8575	Trihedral	240	29.9	134.0	0.2	134.0	0.2	29.8	29.8	134.0	0.0
T1-8	A/D	A/D	46.3453	-84.8497	Trihedral	240	30.2	135.0	0.1	134.0	0.1	29.9	29.9	134.0	0.0
T1-9	A/D	A/D	46.3368	-84.8595	Trihedral	240	29.6	134.0	0.2	135.0	0.2	30.0	30.0	135.0	0.0
T1-10	A/D	A/D	46.3506	-84.8500	Trihedral	240	30.3	135.0	0.3	135.0	0.3	30.1	30.1	135.0	0.0
T2-1	A/D	A/D	46.3337	-84.8593	Trihedral	107	29.9	135.0	0.3	134.0	0.3	29.8	29.8	134.0	0.0
T2-2	A/D	A/D	46.3452	-84.8512	Trihedral	107	29.8	134.0	0.0	134.0	0.0	29.9	29.9	134.0	0.0
T2-3	A/D	A/D	46.3422	-84.8461	Trihedral	107	30.0	135.0	0.1	135.0	0.1	30.0	30.0	135.0	0.0
T2-4	A/D	A/D	46.3406	-84.8457	Trihedral	107	29.7	135.0	0.2	135.0	0.2	29.8	29.8	135.0	0.0
T2-5	A/D	A/D	46.3393	-84.8519	Trihedral	107	29.8	134.0	0.0	134.0	0.0	30.0	30.0	134.0	0.0
T2-6	A/D	A/D	46.3365	-84.8503	Trihedral	107	29.9	134.0	0.2	134.0	0.2	29.9	29.9	134.0	0.0
Raco Airfield	P3	A/D	46.3568	-84.8048	C-PARC #1	44.5	31.8	134.0	0.4	134.0	0.4	21.1	21.1	134.0	0.0
Cryderman	P4	A/D	46.3508	-84.8196	C-PARC #2	42.4	31.8	134.0	0.5	134.0	0.5	21.2	21.2	134.0	0.0
T1-1	A/D	A/D	46.4591	-84.9070	Trihedral	240	30.0	136.0	0.6	136.0	0.6	30.0?	30.0?	136.0?	0.0?
T1-2	A/D	A/D	46.4562	-84.9093	Trihedral	240	30.5	133.5	0.4	133.5	0.4	30.5?	30.5?	133.5?	0.0?
T1-3	A/D	A/D	46.4561	-84.9130	Trihedral	240	29.9	134.0	0.4	134.0	0.4	29.9?	29.9?	134.0?	0.0?
T1-4	A/D	A/D	46.4571	-84.9152	Trihedral	240	30.2	134.5	0.1	134.5	0.1	30.2?	30.2?	134.5?	0.0?
Local Day		Local Date		Friday		30-Sep		15:06:29		Saturday		1-Oct		14:47:51	
Local Time															

table6.formatted

October 1994 Mission									
Launch scheduled for 7:16 am on September 30									
Local magnetic declination is 6.138° W									
Temp (°C) or Level (degrees)	Site	Target Name	Ascending/ Descending	Latitude	Longitude	Target Type	Size (cm)	Max. RCS (dBm*2)	Elevation Angles (From horizontal)
Atten. (dB)	Rifle Range	P1	A/D	46.3481	-84.8487	L-SAPARC		22.2	59.5
0.0	0.0	P2	A/D	46.3369	-84.8519	C-SAPARC		21.9	59.0
0.0	0.3 dB pad	T1-7	A/D	46.3360	-84.8575	Trihedral	240	-	180° off
0.2		T1-8	A/D	46.3453	-84.8497	Trihedral	240	-	180° off
0.1		T1-9	A/D	46.3368	-84.8595	Trihedral	240	-	180° off
0.1		T1-10	A/D	46.3506	-84.8500	Trihedral	240	-	180° off
0.3		T2-1	A/D	46.3337	-84.8593	Trihedral	107	-	180° off
0.1		T2-2	A/D	46.3452	-84.8512	Trihedral	107	-	180° off
0.1		T2-3	A/D	46.3422	-84.8461	Trihedral	107	-	180° off
0.0		T2-4	A/D	46.3406	-84.8457	Trihedral	107	-	180° off
0.0		T2-5	A/D	46.3393	-84.8519	Trihedral	107	-	180° off
0.2		T2-6	A/D	46.3365	-84.8503	Trihedral	107	-	180° off
0.2	Raco Airfield	P3	A/D	46.3568	-84.8048	C-PARC #1	44.5	22.0	239.0
0.6		P4	A/D	46.3508	-84.8196	C-PARC #2	42.4	22.0	240.0
0.67	Cryderman	T1-1	A/D	46.4591	-84.9070	Trihedral	240	-	180° off
0.47		T1-2	A/D	46.4562	-84.9093	Trihedral	240	-	180° off
0.47		T1-3	A/D	46.4561	-84.9130	Trihedral	240	-	180° off
0.17		T1-4	A/D	46.4571	-84.9152	Trihedral	240	-	180° off

table6.formatted

October 1994 Mission										
Launch scheduled for 7:16 am on September 30										
Local magnetic declination is 6.138° W										
All PARCs:										
Elevation Angles (From horizontal)	Azimuth (from true north)	Level (degrees)	Temp (°C) or Atten. (dB)	Site	Target Name	Ascending/ Descending	Latitude	Longitude	Target Type	
31.0	59.0	0.1	1°	Rifle Range	P1	A/D	46.3481	-84.8487	L-SAPARC	
31.2	59.0	yes	4°, 3 dB pad	P2	A/D	46.3369	-84.8519	C-SAPARC		
30.0	59.0	0.1		T1-7	A/D	46.3360	-84.8575	Trihedral	240	
29.6	59.0	0.1		T1-8	A/D	46.3453	-84.8497	Trihedral	240	
29.6	59.5	0.4		T1-9	A/D	46.3368	-84.8595	Trihedral	240	
30.3	60.0	0.3		T1-10	A/D	46.3506	-84.8500	Trihedral	240	
30.2	59.5	0.1		T2-1	A/D	46.3337	-84.8593	Trihedral	107	
30.3	59.0	0.3		T2-2	A/D	46.3452	-84.8512	Trihedral	107	
30.4	59.0	0.6		T2-3	A/D	46.3422	-84.8461	Trihedral	107	
29.8	57.0	0.2		T2-4	A/D	46.3406	-84.8457	Trihedral	107	
29.6	59.0	0.2		T2-5	A/D	46.3393	-84.8519	Trihedral	107	
29.8	59.0	0.1		T2-6	A/D	46.3365	-84.8503	Trihedral	107	
31.0	239.0	0.0		Raco Airfield	P3	A/D	46.3568	-84.8048	C-PARC #1	25.4
31.0	243.0	0.4		P4	A/D	46.3508	-84.8196	C-PARC #2	42.4	
29.9	59.0	0.1		Cryderman	T1-1	A/D	46.4591	-84.9070	Trihedral	240
30.3	59.0	0.0		T1-2	A/D	46.4562	-84.9093	Trihedral	240	
29.9	318.0	0.1		T1-3	A/D	46.4561	-84.9130	Trihedral	240	
30.1	319.0	0.1		T1-4	A/D	46.4571	-84.9152	Trihedral	240	
Wednesday										
5-Oct										
7:22:02										
Local Day										
Local Date										
Local Time										

5
6:15:59
86
D
N
24.432
25.367
131.411
311.862
S
318

5
6:15:59
86.4
Data-Take No.
Ascending/Descending
North/South Looking (from Shuttle)
Look Angle (relative to SIR-C)
Local Incidence Angle
SIRC Azimuth Heading (True North)
Target Azimuth (True North)
Target Looking (N/S)
Target Azimuth (Mag. North)

5
25.4
Elevation Angles
(From horizontal)

5
Azimuth (from
true north)

table6.formatted

table6.formatted

table6.formatted

Size (cm)	Max. RCS (dBm \times 2)	Elevation Angles (From horizontal)		Temp (°C) or Atten. (dB)	Azimuth (from true north)	Level (degrees)	Elevation Angles (From horizontal)	Azimuth (from true north)	Level (degrees)	Temp (°C) or Atten. (dB)	Site	Target Name	Ascending/ Descending	Latitude	
		AirSAR	AirSAR												
240	41.2 (31.5 AirSAR)	316.5 (318 AirSAR)	0.0	18° (20° AirSAR)	41.2 (42.7 AirSAR)	318.0	0.0	41.2 (42.7 AirSAR)	318.0	0.0	18° SIR-C (15°, 3 dB pad AirSAR)	P1	A/D	46.3481	
240	10.1	318.0	yes	3dB pad (22°, 2 dB pad AirSAR)	41.2 (42.7 AirSAR)	318.0	0.0	41.2 (42.7 AirSAR)	318.0	0.0	15° SIR-C (15°, 3 dB pad AirSAR)	P2	A/D	46.3369	
240	-	-	0.1	-	10.0	318.0	0.1	-	-	-	-	T1-7	A/D	46.3360	
240	10.0	318.0	0.1	-	-	318.0	0.1	-	-	-	-	T1-8	A/D	46.3453	
240	-	-	-	-	9.9	317.5	0.0	-	-	-	-	T1-9	A/D	46.3368	
240	-	-	-	-	-	318.0	0.6	-	-	-	-	T1-10	A/D	46.3506	
107	-	-	-	-	-	318.0	0.0	-	-	-	-	T2-1	A/D	46.3337	
107	-	-	-	-	9.5	318.0	0.2	-	-	-	-	T2-2	A/D	46.3452	
107	10.0	318.0	0.0	-	-	318.0	0.0	-	-	-	-	T2-3	A/D	46.3422	
107	-	-	-	-	9.9	318.0	0.1	-	-	-	-	T2-4	A/D	46.3406	
107	9.9	318.0	0.0	-	-	318.0	0.2	-	-	-	-	T2-5	A/D	46.3393	
107	10.0	318.0	0.1	-	9.8	318.0	0.0	-	-	-	-	T2-6	A/D	46.3365	
44.5	41.2	318.0	0.5	-	41.2	318.0	0.1	-	-	-	-	P3	A/D	46.3568	
42.4	41.2	318.0	0.5	-	41.2	318.0	0.7	-	-	-	-	P4	A/D	46.3508	
240	9.9	59.0	0.1	-	10.3	318.0	0.1	-	-	-	-	Cryderman	T1-1	46.4591	
240	10.6	59.0	0.1	-	10.0	318.0	0.1	-	-	-	-	T1-2	A/D	46.4562	
240	29.5	318.0	0.1	-	10.0	318.0	0.1	-	-	-	-	T1-3	A/D	46.4561	
240	33.3	322.0	1.4	-	10.0	318.0	0.2	-	-	-	-	T1-4	A/D	46.4571	
													Saturday		
													8-Oct		
													12:29:40		
													AirSAR Data		
													Local Day		
													Local Date		
													Local Time		

table6.formatted

MET (dd)	9	MET (hh:mm:ss)	4:51:57	Temp (°C)	10
Orbit No.	150				4:30:20
Date-Take No.	150.2				166.1
Ascending/Descending	D				D
North/South Looking (from Shuttle)	N				N
Look Angle (relative to SIR-C)	39.596				39.596
Local Incidence Angle	41.248				41.248
SIRC Azimuth Heading (True North)	132.424				132.424
Target Azimuth (True North)	311.862				311.862
Target Looking (N/S)	S				S
Target Azimuth (Mag. North)	318				318
Longitude	Target Type	Size (cm)	Max. RCS (dBm^2)	Elevation Angles (From horizontal)	Elevation Angles (From horizontal)
-84.8487	L-SAPARC			41.2	318.0
					0.0
					41.2
					318.0
					0.0
-84.8519	C-SAPARC			41.2	318.0
					0.1
					5°
					41.2
					318.0
-84.8575	Trihedral	240	321.5	0.3	10.3
-84.8497	Trihedral	240	317.5	0.0	9.9
-84.8595	Trihedral	240	317.5	0.1	10.1
-84.8500	Trihedral	240	316.0	0.1	10.6
-84.8593	Trihedral	107	316.0	0.1	10.0
-84.8512	Trihedral	107	317.5	0.1	9.9
-84.8461	Trihedral	107	318.0	0.0	10.0
-84.8457	Trihedral	107	318.0	0.2	10.0
-84.8519	Trihedral	107	318.0	0.2	9.9
-84.8503	Trihedral	107	318.0	0.1	9.9
-84.8048	C-PARC #1	44.5	41.2	318.0	0.4
-84.8196	C-PARC #2	42.4	41.2	318.0	0.9
-84.9070	Trihedral	240	10.0	318.0	0.2
-84.9093	Trihedral	240	10.1	318.0	0.1
-84.9130	Trihedral	240	10.0	318.0	0.1
-84.9152	Trihedral	240	10.0	318.0	0.1
					10.1
					318.0
					0.0
					Monday
					9-Oct
					12:07:57
					AirSAR Data

3 SUMMARY OF ACCOMPLISHMENTS

As mentioned, accurate calibration of polarimetric imaging radars involves many steps. Towards this goal, we have focused our activities in four areas: (1) development of calibration algorithms for the purpose of characterizing the scattering matrices of the SAR calibration targets, (2) design and characterization of precision calibration targets, (3) development of a calibration technique for measurement of differential Mueller matrices of distributed targets which is required for cross calibration and calibration methods based on known distributed targets, and (4) development of calibration algorithms for imaging radars. A summary of the work accomplished in each area is given next.

3.1 Calibration Algorithms For Point Targets

Three distinct algorithms have been developed for the measurement of scattering matrices of point targets. Our objective in the development of these algorithms was to characterize the scattering matrices of SAR calibration targets with a high degree of accuracy by comparing them against a precision metallic sphere. The choice of the calibration algorithm depends on the particular system and the accuracy-versus-complexity criterion. For example, in the calibration technique which will be referred to as IACT (isolated antenna calibration technique) only a metallic sphere and any other target with relatively high cross-polarized component are required to determine the radar distortion parameters [4]. The scattering matrix of the depolarizing target need not be known. This technique is very convenient, however it is only applicable to radar systems with low cross-talk. Refer to Appendix B for a detailed explanation of the procedure.

Another calibration technique that is not based on any *a priori* knowledge of the system was also developed [4]. In this technique the transmit and receive distortion matrices of the radar system are characterized using three independent targets with known scattering matrices. Although this method is very general, its drawback is the errors caused by orienting the calibration targets with respect to the antenna system coordinate frame (see Appendix B). Using the property of reciprocal passive antennas, a convenient calibration technique was later developed that determines the distortion parameters of a radar system using only a metallic sphere [5]. This technique will be referred to as STCT (single target calibration technique). Using this calibration technique the scattering matrix elements of a target can be measured with an accuracy of 0.5 dB in magnitude and ± 5 degrees in phase. The calibration procedure is described in Appendix B.

3.2 Measurement and Calibration of Differential Mueller Matrices

The overall accuracy of a calibration procedure for imaging radars can be assessed if an independent accurate measurement of an area within the image were available. With this purpose in mind, we developed an algorithm for backscatter measurement of uniform distributed targets using a scatterometer system. A major difficulty in the Mueller matrix measurement of distributed targets is the lack of known distributed targets, and therefore the calibration coefficient must be inferred from point calibration targets. This process is rather complex, particularly when the radar distortions vary over the illuminated area. This is the case when a scatterometer is used for the measurement. Amplitude and phase variation of the radiation pattern of the scatterometer antenna causes variation in the distortion parameters of the radar over its illuminating area. In this case the distortion parameters must be determined over the entire main beam of the radar system using point calibration targets in order to find the calibration coefficient for distributed targets [6].

Using this procedure, the differential Mueller matrix of an area can be determined, which in turn can be used to calibrate a polarimetric SAR. In such a calibration technique, it can be shown that the impulse response of the SAR (ambiguity function) need not be determined. The detailed procedure and experimental results of the Mueller matrix measurement is given in Appendix C.

3.3 Characterization and Design of Precision Active Calibration Targets

There are significant differences between point calibration targets used for conventional radars and imaging radars. These differences are the direct result of the target deployment configuration. For imaging radars, the calibration targets are placed on the ground (in the presence of the distributed target), whereas in the case of conventional radars the calibration targets are placed in free space. The success of an external calibration procedure relies on the knowledge of the scattering matrix of the calibration targets. In order to reduce the effect of background (direct contribution) on the RCS of a calibration target for imaging radars, it is required that the RCS of the target be much larger than that of the surrounding background.

Calibration targets, in general, can be categorized into two major groups: (1) passive calibrators and (2) active calibrators [7]. Passive calibrators are more stable and reliable than their active counterparts, however, their large physical dimensions is their major drawback. Trihedral corner reflectors are the most widely used targets for imaging radars because of their high RCS and wide RCS pattern. In recent years, polarimetric active radar calibra-

tors (PARC's) have been used extensively and are planned to be employed for external calibration of the SIR-C/XSAR mission. In addition to high RCS and wide RCS pattern, PARC's are desirable for their relatively small physical size. In June 1990, the scattering matrices of JPL L- and C-band PARC's were measured and the results were reported [8]. The measurements were conducted over a wide range of incidence angles in azimuth, elevation, 45°, and 135° planes. It was found that the RCS patterns of the L-band PARC's whose antennas were in close proximity, were unsymmetric and the phase patterns exhibited rapid fluctuations. These undesirable characteristics prompted design of a novel single antenna PARC (see Appendix D). The new PARC can provide a very high RCS while having a relatively small physical size. We are currently in the process of manufacturing two L-band and two C-band single antenna PARCs (SAPARC). The features and performance characteristics of a C-band SAPARC was reported [9].

3.4 Analysis, Design, and Construction of an Optimum Corner Reflector

PARC's are excellent calibration targets in regard to large RCS and wide RCS pattern requirements. However, the scattering matrix of a PARC is singular and can only provide three equations for the unknown distortion parameters of a radar instead of four [10]. Besides, in order to check the validity of a calibration algorithm, independent known targets are required. Trihedral corner reflectors are suitable for this purpose. Large ordinary trihedrals are not very reliable for calibration. The frame of these trihedrals are not sturdy enough and causes geometrical deformations. Obviously construction of a sturdy trihedral with such large dimensions renders them practically undeployable. The other problem is the coherent interaction of the trihedral with the ground. The reflected wave from the surface in front of the trihedral scatters off of the lower panel edge and returns to the radar. Also rays from the scatterers on the ground may enter the trihedral cavity and reflect back towards the radar. Basically, the image of these scatterers in the trihedral are visible. This interaction occurs with the upper portion of the side panels. The significance of this interaction depends on the tilt angle of the lower panel, since the lower panel can shadow some of the scatterers in front of the trihedral RCS analysis of trihedral corner reflectors shows that only a portion of the trihedral is contributing to the RCS. A new class of corner reflectors that does not suffer from the aforementioned problems were designed and constructed. These corner reflectors are suitable for calibration of imaging radar systems [11] (also see Appendix E).

3.5 Calibration Algorithms for Polarimetric SAR Systems

We have developed two approaches for calibration of polarimetric synthetic aperture radars. The first approach is based on point calibration targets [12]. In this method the polarimetric ambiguity function of the SAR is estimated from a trihedral in the image and using a model similar to the one used in STCT, the calibration constant and distortion parameters of the SAR can be obtained. Accuracy of this calibration directly depends on the knowledge of the scattering matrix of the trihedral calibration target. The detailed procedure and actual implementation of this technique is given in Appendix F. In the second approach a uniform distributed target is used as a calibration target [13]. The differential Mueller matrix of this target can be characterized using the scatterometer systems, and the radar distortion parameters and the calibration constant can be obtained directly from this algorithm. The outcome of this calibration algorithm is the calibrated differential Mueller matrices of the uniform regions in the image. The advantages offered here are as follows: (1) point targets are not needed and the calibration is not influenced by the interaction of the targets with their backgrounds, (2) estimation of polarimetric ambiguity function is not required, (3) since the differential Mueller matrix is calculated from many independent measurements the effect of noise and measurement errors are minimized. In Appendix F this procedure is explained in detail.

3.6 Cross Calibration Experiment

In June 1991 a cross calibration experiment using JPL AirSAR and the University of Michigan scatterometer system was conducted to assess the accuracy of SAR calibration using point targets. The results of this experiment is reported in Appendix G. Four different uniform distributed targets, three rough surfaces with different roughness and a hay field, were measured with both the scatterometers and the JPL SAR at three different incidence angles. After processing the data, significant discrepancies between the two measurements were observed . Two factors are believed to be responsible for these discrepancies, both related to the trihedrals used in the experiment. One is the effect of coherent and incoherent interaction of the ground with the trihedrals. These factors affect the scattering matrix of the trihedrals used in the calibration. The second factor is the possible geometrical deformation of the trihedrals.

3.7 Applications

In the past two years we have examined the applications of calibrated polarimetric SARs in radar remote sensing of vegetation. First high fidelity scattering models for short vegetation was developed [13,14] and then inver-

sion algorithms were developed and physical parameters of vegetation were retrieved from calibrated polarimetric SARs [14,15]. Appendix II includes copies of these papers.

4 Students Supported

Throughout the course of this investigation the effort of the following Ph.D. and M.S. students were supported fully or partially by this project.

Ph.D. Students

1. Michael Whitt
2. Yisok Oh
3. Tsenchieh Chiu
4. Jim Stiles
5. Roger DeRoo

M.S. Students

1. M. Ali Tassoudji
2. James Ahne
3. A. Zambetti

5 Publications

Journal Publications:

1. Sarabandi, K., F.T. Ulaby, and M.A. Tassoudji, "Calibration of polarimetric radar systems with good polarization isolation", *IEEE Trans. Geosci. Remote Sensing*, vol. 28, no. 1, Jan. 1990.
2. Whitt, M.W., and F.T. Ulaby, "A polarimetric radar calibration technique with insensitivity to target orientation," *Radio Sci.*, vol. 25, no. 6., pp. 1137-1143, 1990.
3. Whitt, M.W., F.T. Ulaby, P. Polatin, V.V. Liepa, "A general polarimetric radar calibration technique: Theory and experiment," *IEEE Trans. Antennas Propagat.*, vol. 39, no. 1, Jan. 1991.

4. Sarabandi, K., and F.T. Ulaby, "A convenient technique for polarimetric calibration of radar systems", *IEEE Trans. Geosci. Remote Sensing*, vol. 28, no. 6, Nov. 1990.
5. Sarabandi, K., Y. Oh, and F.T. Ulaby, "Measurement and calibration of differential Mueller matrix of distributed targets," *IEEE Trans. Antennas Propagat.*, vol. 40, no. 12, pp.1524-1532, Dec. 1992.
6. Sarabandi, K., Y. Oh, and F.T. Ulaby, "Application and performance characterization of polarimetric active radar calibrator", *IEEE Trans. Antennas Propagat.*, vol. 40, no. 10, Oct. 1992.
7. Sarabandi, K., L.E. Pierce, and F.T. Ulaby, "Calibration of a polarimetric imaging SAR", *IEEE Trans. Geosci. Remote Sensing*, vol. 30, no. 3, May 1992.
8. Sarabandi, K., "Calibration of a polarimetric synthetic aperture radar using a known distributed target" *IEEE Trans. Geosci. Remote Sensing*, vol. 32, no. 3, 575-582, May 1994.
9. Sarabandi, K., L. Pierce, M.C. Dobson, F.T. Ulaby, J. Stiles, T.C. Chiu, R. De Roo, R. Hartikka, A. Zambetti, and A. Freeman, "Polarimetric calibration of SIR-C using point and distributed targets," *IEEE Trans. Antennas Propagat.*, vol. 33, no. 4, pp. 858-866, July 1995.
10. Freeman, A., M. Alves, B. Chapman, J. Cruz,, Y. Kim, S. Shaffer, J. Sun, E. Turner, and K. Sarabandi, "SIR-C Calibration Results," *IEEE Trans. Geosci. Remote Sensing*, vol. 33, no. 4, pp. 848-857, July 1995.
11. Sarabandi, K., and T.C. Chiu, "An optimum corner reflector for calibration of imaging radars," *IEEE Trans. Antennas Propagat.*, vol. 44, no. 10, Oct. 1996.
12. Chiu, T.C., and K. Sarabandi, "Electromagnetic Scattering from Short Branching Vegetation," *IEEE Trans. Geosci. Remote Sensing*, submitted for publication (Jan. 98).
13. Chiu, T.C., and K. Sarabandi, "Electromagnetic scattering interaction between a dielectric cylinder and a slightly rough surface," *IEEE Trans. Antennas Propagat.*, submitted for publication (June 1997).
14. Svendsen, M.T., K. Sarabandi, and H. Skriver, "Retrieval of vegetation parameters from SAR data using a coherent scattering model for grassland," *IEEE Trans. Geosci. Remote Sensing*, submitted for publication (April 99).

Conference Papers:

1. M.T. Svendsen, and K. Sarabandi, "Retrieval of vegetation parameters from SAR data using a coherent scattering model for grassland," *Proc. 2nd Int. Workshop on Retrieval of Bio- and Geo-physical Parameters from SAR data for Land Appl.*, Noordwijk, Netherlands, 21-23 Oct., 1998. (invited)
2. T. Chiu and K. Sarabandi, "Electromagnetic scattering interaction between leaves and thin branches," *Proc. IEEE Trans. Geosci. Remote Sensing Symp.*, Seattle, 1998.
3. T. Chiu and K. Sarabandi, "A coherent second-order scattering model for short vegetation," *Proc. IEEE Trans. Geosci. Remote Sensing Symp.*, Seattle, 1998.
4. Y. Kobayashi, K. Sarabandi, L. Pierce, M.C. Dobson, "Extracting Tree Heights using JPL TOPSAR DEM data," *Proc. IEEE Trans. Geosci. Remote Sensing Symp.*, Seattle,
5. Chiu, T.C., and K. Sarabandi, "Electromagnetic scattering interaction between a dielectric cylinder and a slightly rough surface," *Proc. IEEE Trans. Geosci. Remote Sensing Symp.*, Singapore, 1997.
6. Sarabandi, K., and T.C. Chiu, "Optimum corner reflectors design," *Proc. IEEE National Radar Conference*, Ann Arbor, Michigan, May 1996.
7. Sarabandi, K., L. Pierce, M.C. Dobson, T.C. Chiu, F.T. Ulaby, and J. Stiles, "Polarimetric calibration of SIR-C using point and distributed targets," *Proc. IEEE Trans. Geosci. Remote Sensing Symp.*, Firenze, Italy, July 1995.
8. Sarabandi, K., and T.C. Chiu, "Optimum corner reflectors for calibration of Imaging radars," *Proc. IEEE Trans. Geosci. Remote Sensing Symp.*, Firenze, Italy, July 1995.
9. Sarabandi, K., and Y. Oh, "Effect of antenna footprint on the statistics of radar backscattering ,"*Proc. IEEE Trans. Geosci. Remote Sensing Symp.*, Firenze, Italy, July 1995.
10. Sarabandi, K., and A. Nashashibi, "A novel bistatic scattering matrix measurement technique using a monostatic radar," Presented at AP/URSI symposium, Seattle, June 1994.
11. Freeman, A., A. Azeem, D. Haub, and K. Sarabandi, "Development of SIR-C ground calibration equipment," Presented at SAR Calibration Workshop, Noordwijk, The Nether Lands, Sept. 1993.

12. Sarabandi, K., J. Ahne, F. Ulaby, and A. Freeman, "Single-antenna polarimetric active radar calibrators for the SIR-C Mission," Presented at SAR Calibration Workshop, Noordwijk, The Nether Lands, Sept. 1993.
13. Sarabandi, K., F.T. Ulaby, M.C. Dobson, "AIRSAR and POLARSCAT cross-calibration using point and distributed targets," presented at IGARSS'93, Tokyo, 1993.
14. Ahne, J. J., K. Sarabandi, and F.T. Ulaby, "Design and implementation of single antenna polarimetric active radar calibrators," *Proc. IEEE Trans. Antennas Propagat. Symp.*, Ann Arbor, 1993.
15. Dobson, M.C., K. Sarabandi, L. Pierce, and F.T. Ulaby, "External calibration of ERS-1 SAR," presented at IGARSS'92, Houston, May 1992.
16. Sarabandi, L.E. Pierce, Y. Oh, M.C. Dobson, A. Freeman, and P. Dubois, "Cross calibration experiment using JPL AIRSAR and truck-mounted polarimetric scatterometers," presented at IGARSS'92, Houston, May 1992.
17. Sarabandi, K., L.E. Pierce, and F.T. Ulaby, "Calibration of a polarimetric imaging SAR", *JPL Airborne Geosci. Workshop*, Pasadena, May 1991.
18. Sarabandi, K., Y. Oh, and F.T. Ulaby, " Application and performance characterization of polarimetric active radar calibrator", *JPL Airborne Geosci. Workshop*, Pasadena, May 1991.
19. Sarabandi, K., and F.T. Ulaby, "A convenient technique for polarimetric calibration of radar systems", *Proc. IEEE Trans. Geosci. Remote Sensing Symp.*, Maryland, May 1990.
20. Sarabandi, K., F.T. Ulaby, M.W. Whitt, and P. Polatin, "Comparison of several polarimetric radar calibration techniques", *Proc. International Union of Radio Science*, Hyannis, May 1990.
21. Liepa, V.V., K. Sarabandi, and M.A. Tassoudji, " A pulsed network analyzer based scatterometer", *Proc. of IEEE Geosci. Remote Sens. Symp.*, Vancouver, July 1989.
22. Sarabandi, K., and F.T. Ulaby, "Calibration of polarimetric radar systems". *Proc. of IEEE Geosci. Remote Sens. Symp.*, Vancouver, July 1989. 1998.

References

- [1] Sarabandi, K., L. Pierce, M.C. Dobson, F.T. Ulaby, J. Stiles, T.C. Chiu, R. De Roo, R. Hartikka, A. Zambetti, and A. Freeman, "Polarimetric calibration of SIR-C using point and distributed targets," *IEEE Trans. Antennas Propagat.*, vol. 33, no. 4, pp. 858-866, July 1995.
- [2] Freeman, A., M. Alves, B. Chapman, J. Cruz,, Y. Kim, S. Shaffer, J. Sun, E. Turner, and K. Sarabandi, "SIR-C Calibration Results," *IEEE Trans. Geosci. Remote Sensing.*, vol. 33, no. 4, pp. 848-857, July 1995.
- [3] Sarabandi, K., F.T. Ulaby, and M.A. Tassoudji, "Calibration of polarimetric radar systems with good polarization isolation", *IEEE Trans. Geosci. Remote Sensing.*, vol. 28, no. 1, Jan. 1990.
- [4] Whitt, M.W., F.T. Ulaby, P. Polatin, V.V. Liepa, "A general polarimetric radar calibration technique: Theory and experiment," *IEEE Trans. Antennas Propagat.*, vol. 39, no. 1, Jan. 1991.
- [5] Sarabandi, K.. and F.T. Ulaby, " A convenient technique for polarimetric calibration of radar systems", *IEEE Trans. Geosci. Remote Sensing.*, vol. 28, no. 6, Nov. 1990.
- [6] Sarabandi, K., Y. Oh, and F.T. Ulaby, "Measurement and calibration of differential Mueller matrix of distributed targets," *IEEE Trans. Antennas Propagat.*, vol. 40, no. 12, pp.1524-1532, Dec. 1992.
- [7] Brunfeldt, D.R., and F.T. Ulaby, "Active calibrators for radar calibration ,," *IEEE Trans. Geosci. Remote Sensing*, vol 22, no 2, 1984.
- [8] Sarabandi, K., and Y. Oh, "RCS measurement of polarimetric active radar calibrators.", *Radiation Laboratory Report No. 027165-1-T* , The University of Michigan, June 1990.
- [9] Ahne, J.J, K. Sarabandi, F.T. Ulaby, "Design and implementation of a C-band single antenna polarimetric active radar calibrator," *Radiation Laboratory Report No. 027587-1-T* , The University of Michigan. August 1993.
- [10] Sarabandi, K.. Y. Oh, and F.T. Ulaby, " Application and performance characterization of polarimetric active radar calibrator", *IEEE Trans. Antennas Propagat.*, vol. 40, no. 10, Oct. 1992.
- [11] Sarabandi, K., and T.C. Chiu," An optimum corner reflector for calibration of imaging radars," *IEEE Trans. Antennas Propagat.*, vol. 44, no. 10, Oct. 1996.

- [12] Sarabandi, K., L.E. Pierce, and F.T. Ulaby, "Calibration of a polarimetric imaging SAR", *IEEE Trans. Geosci. Remote Sensing.*, vol. 30, no. 3, May 1992.
- [13] Sarabandi, K., "Calibration of a polarimetric synthetic aperture radar using a known distributed target" *IEEE Trans. Geosci. Remote Sensing.*, vol. 32, no. 3, 575-582, May 1994.

APPENDIX A

RESULTS OF SIR-C/XSAR EXPERIMENTS